Received: 17 April 2025 | Revised: 3 October 2025 | Accepted: 7 October 2025

DOI: 10.1002/dep2.70052

The Depositional Record
Open Access
A journal of the International Association of Sedimentologists
WILEY

ORIGINAL ARTICLE

Laguna Fuente de Piedra: An example of a dolomite factory recording ~50,000 years of depositional and paleoclimatic evolution

Zeina Naim[1] | **Guolai Li**[1] | **Luis Gibert**[2] | **Jan-Berend Stuut**[1,3] | **Gonzalo Jiménez-Moreno**[4] | **Mónica Sánchez-Román**[1,5]

[1]Earth Sciences Department, Science Faculty, Vrije Universiteit Amsterdam, Amsterdam, the Netherlands

[2]Mineralogy, Petrology and Applied Geology Department, University of Barcelona, Barcelona, Spain

[3]NIOZ, Royal Netherlands Institute for Sea Research, Texel, The Netherlands

[4]Stratigraphy and Palaeontology Department, Sciences Faculty, University of Granada, Granada, Spain

[5]Mineralogy and Petrology Department, Sciences Faculty, University of Granada, Granada, Spain

Correspondence
Zeina Naim and Mónica Sánchez-Román, Earth Sciences Department, Science Faculty, Vrije Universiteit Amsterdam, de Boelelaan 1085, 1081HV, the Netherlands.
Email: z.naim@vu.nl and m.sanchezroman@ugr.es

Funding information
Nederlandse Organisatie voor Wetenschappelijk Onderzoek, Grant/Award Number: OCENW.KLEIN.037

Abstract

We examine the depositional dynamics and paleoclimatic significance of the evaporite–dolomite association in Laguna Fuente de Piedra (LFP), a modern saline, endorheic playa lake system in southern Spain. This study presents results from a multidisciplinary approach, examining the two longest continuous sediment cores retrieved from the basin. One core was drilled in the Salina area, located in the eastern part of the basin, which represents the zone that dries last and is referred to as the Salina core (14.4 m). The second core, Las Latas (46.2 m), was retrieved from the southwestern part of the basin, which is the zone that dries first. This study characterises carbonate minerals and their precipitation mechanism in the sediments from these two cores over the past ~50,000 years. Six major lithofacies were identified based on variations in mineralogy (carbonates, sulphates and siliciclastic minerals) and sedimentary patterns. Observed shifts in the depositional environment are hypothesised to result from changes in the hydrological balance, which in turn is controlled by paleoclimatic evolution. During dry and cold periods, the basin experienced higher evaporation rates, leading to the deposition of evaporites along with dolomite in a continental sabkha environment with ephemeral floods. These arid conditions favoured large production of endogenic sulphates and carbonates (dolomite) and reduced clastic input. In contrast, wetter periods were characterised by increased clastic influx and the precipitation of calcite–aragonite facies, in a shallow ephemeral to permanent lake, mostly during the Pleistocene–Holocene transition, continuing into the Holocene. These findings show the high sensitivity of shallow continental sedimentary systems to climate variations and provide information on significant short-lived climatic events, tentatively correlated with Heinrich events, in the western Mediterranean region.

KEYWORDS

arid, continental sabkha, dolomite, EPS, playa lake, western Mediterranean

1 | INTRODUCTION

Climatic shifts during the Quaternary period have significantly influenced both continental and coastal environments, altering depositional dynamics. The Iberian Peninsula, with its diverse climatic regimes ranging from the humid Atlantic coast to the semi-arid and arid Mediterranean interior, provides a valuable setting for investigating these environmental changes (Camuera et al., 2022; Combourieu Nebout et al., 2009; Martrat et al., 2004; Rodrigo-Gámiz et al., 2011). In particular, the formation and evolution of saline playa lake systems within endorheic basins serve as key archives for reconstructing past climatic and hydrological conditions.

Modern environments where dolomite [Ca, $Mg(CO_3)_2$] formation predominantly occurs include coastal and inland sabkhas as well as coastal lakes and playa lakes. Among these, sabkhas have received remarkable attention, mainly within sedimentology and geochemistry fields due to the occurrence of modern dolomite precipitation (e.g. DiLoreto et al., 2019, 2021; Rosen et al., 1989; Sánchez-Román et al., 2023; Warren, 2000) as well as, to a lesser extent, playa lakes (e.g. De Deckker & Last, 1988, 1989). Eugster (1982) highlights the importance of playa lake deposits and evaporites as indicators of local climate. Consequently, the mineralogical and geochemical characteristics of playa lake systems have gained attention in recent years, particularly in paleoenvironmental and paleoclimatic research, as highlighted by Pourali et al. (2023).

The semi-arid climate of SE Spain, coupled with widespread endorheic basins, has facilitated the development of numerous playa lakes in this region. However, a comprehensive understanding of the mechanisms driving carbonate deposition and the paleoenvironmental significance of evaporite–dolomite associations in these systems remains incomplete. To refine depositional models and reconstruct past environmental conditions, an integrated approach combining sedimentology, petrography, mineralogy and geochemistry is required.

Several paleoclimatic studies have been conducted on saline lakes in southern Spain, including Laguna Salada (Schröder et al., 2018a), Laguna de Medina (Reed et al., 2001; Schroeder et al., 2018b), Laguna de Salines (Burjachs et al., 2016; Giralt et al., 1999), Laguna de la Ballestera (García-Alix et al., 2022), Laguna de Zónăr (Martín-Puertas et al., 2008) and on short cores from Laguna Fuente de Piedra (LFP; Höbig et al., 2016). While these studies have provided valuable insights, the available terrestrial archives spanning the last glacial cycle remain relatively limited compared to other regions of the Iberian Peninsula. This limitation is primarily due to the scarcity of long enough sedimentary records. Additionally, challenges in establishing precise age control have led to gaps or discontinuities in the records. A previous study in LFP examined a 14-m core, which provided a sedimentary record from the margin of the basin extending over the past 30 cal kyr (Höbig et al., 2016). These authors described five distinctive lacustrine lithofacies along with fluvial deposits and developed a conceptual lake margin model in which recurring lake-level fluctuations influenced the occurrence of these lithofacies throughout the sedimentary succession.

The present study builds upon the work of Höbig et al. (2016) by expanding the LFP sedimentary archive with two cores, 46.2 m and 14.4 m, drilled in more central areas of the basin. In this context, the multiproxy record from LFP offers a unique opportunity to expand the paleoclimatic history of the region and investigate the environmental conditions controlling carbonate precipitation. This study integrates sedimentology, mineralogy, geochemistry, palynology and microscopy to (1) characterise the sedimentary facies, with a focus on the mechanisms driving the precipitation of aragonite, calcite and dolomite; (2) assess the paleoclimatic significance of evaporite-dolomite associations in playa lake systems; and (3) evaluate the regional paleoclimatic evolution. Our findings will contribute to a better understanding of the climatic and hydrological controls on carbonate deposition in saline lake environments and provide new insights into Quaternary climate variability in the western Mediterranean.

2 | GEOLOGICAL SETTING

LFP is an arid, saline, isolated playa lake system located in Antequera (southern Spain), approximately 60 km northwest of Málaga city (Figure 1A,B). LFP is located in an intramontane endorheic basin with a 150 km^2 watershed area within the Betic Cordillera, which developed as a result of late orogenic tectonic extension processes during the Neogene period (Kohfahl et al., 2008). Outcrops of the Triassic gypsum forming part of the Antequera unit are exposed in the area (Calaforra & Pulido-Bosch, 1999; Lhénaff, 1981). The karstification of these evaporitic deposits was interpreted as a probable origin of LFP (Montalván et al., 2017).

LFP, with a surface area of approximately 13.5 km^2, lies in a topographically shallow, closed basin, and is a playa lake with seasonal standing water. During summer, desiccation leads to the precipitation of a salt crust, which later dissolves with the first rains in autumn. The lake is known to be an important natural reserve as it is a nesting site for one of the largest flamingo colonies (*Phoenicopterus roseus*) in the western Mediterranean.

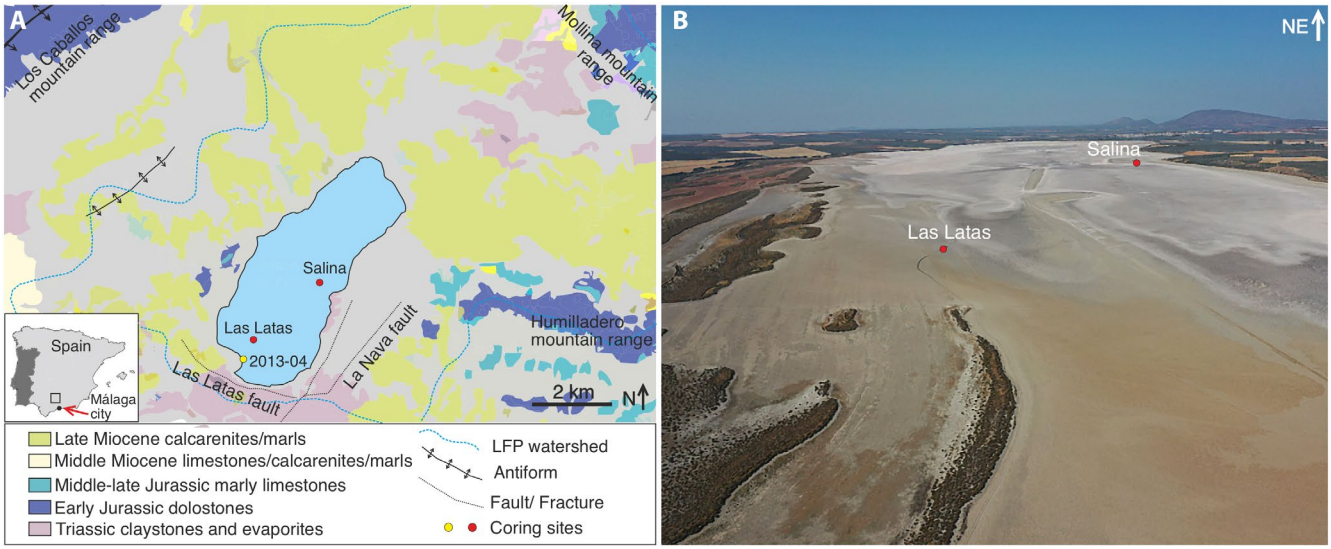

FIGURE 1 (A) Geological map of Laguna Fuente de Piedra (LFP) showing the main stratigraphic units and tectonic features (adapted from Jiménez-Bonilla et al., 2024; Rodríguez-Rodríguez et al., 2005). (B) Drone photograph of LFP taken in July 2021, highlighting dry-season conditions where the playa lake is covered with a greyish-white salt crust and beige-orange microbial mats (in the southeastern part).

In this regard, it was the first Spanish wetland included in the Ramsar Agreement (Girela & Martos, 1998; Heredia et al., 2004).

The playa lake is bounded by two mountain ranges, the Mollina (NE) and Humilladero (E) Ranges. They are composed of Jurassic with minor Cretaceous marly and cherty limestones, and dolostones constituting the main karstic outcrops in the area (Höbig et al., 2016; Rodríguez-Rodríguez et al., 2006, 2016). The playa lake is also bounded by La Nava (sinistral-normal fault) and the Las Latas (dextral-normal fault) at the eastern and southern margins of LFP, respectively (Jiménez-Bonilla et al., 2024). Moreover, the LFP Basin is located in an ellipsoidal closed depression included in the so-called synorogenic mélange unit that is mainly composed of Triassic claystones and evaporites embodied within Jurassic, Cretaceous and Tertiary disorganised blocks (Pedrera et al., 2016; Sanz de Galdeano et al., 2008).

Numerous studies have investigated the hydrology of LFP due to its relevance in understanding the local ecosystem dynamics. Rodriguez-Rodriguez et al. (2016) provided an overview of the hydrogeology of the lake. While precipitation and several ephemeral streams contribute to the lake's water input, the predominant hydrological source is groundwater. Kohfahl et al. (2008) described a conceptual model with two primary types of groundwater flow systems: (i) meteoric groundwater from the north and south edges of the basin orientated towards the lake; (ii) a second system developed below the surface of the playa lake by convection processes and evapotranspiration. Recycled brines that result from mixing at the interface of the convection cells with freshwater discharge are subsequently transported upwards to the playa lake. This model was proposed as the most plausible conceptual model for LFP's hydrological system by Rodriguez-Rodriguez et al. (2016). The high water salinity range in the playa lake results from the interaction with, and leaching of, Triassic evaporites by both surface run-off and groundwater. The primary cation in the lake water chemistry is Na^+, with Mg^{2+} and Ca^{2+} present in lower concentrations. The main anion is Cl^-, with SO_4^{2-} also present in noticeable concentrations (Rodríguez-Rodríguez et al., 2005).

3 | MATERIALS AND METHODS

3.1 | Coring site and recovery

Two sediment cores from LFP were retrieved in July 2021: the Salina core (14.4 m) from the mid-eastern depocenter of the lake and the Las Latas core (46.2 m) from the southern margin of the lake (Figure 1B). The drilling campaign was carried out by Centro de Instrumentation Cientifica (Spain) using a Rolatec RL 48 L drilling rig with a rotation head, speed from 0 to 900 rpm, variable control, maximum torque 450 kgm, with an opening leaving the drilling area free. The continuous cores were recovered using two methods: (1) percussion, in which the sediment is directly collected into PVC tubes, and (2) rotation, where the cores were collected without tubing and were later transferred to PVC tubes. After transport

to the Vrije Universiteit Amsterdam (The Netherlands), 60 cm sections of the drill cores were split longitudinally with a wire. The cores were described based on lithology, mineralogy, and fossil content. Lithofacies characterisation also considered sedimentary textures, structures and colour, which are standard indicators for environmental interpretation (Reading, 2009). The drill cores were later stored horizontally at 4°C.

3.2 | Radiocarbon dating

The age model of the 46.2 m sedimentary record from the Las Latas core is based on a combination of newly acquired ^{14}C ages and previously published radiocarbon data by Höbig et al. (2016) (Table 1, Figure 2). The latter ages were derived from a 14-m core (2013-04) retrieved from the southwestern part of the lake, approximately 600 m from the Las Latas site. The samples from Höbig et al. (2016) included a mixture of pollen, wood and bulk sediments, whereas the new radiocarbon dates from the Las Latas core were obtained on bulk sediments. Although the lithofacies in the two cores are not identical, the recurring sedimentary patterns with a significant increase in calcite in both cores at approximately the same depth allowed a reliable correlation. This correlation supports the upper part of the age model and is illustrated in Figure S1.

The upper 13.7 m of the Las Latas core incorporates four data points from the age model of Höbig et al. (2016), while 10 additional radiocarbon samples were analysed in the Poznan Radiocarbon Laboratory (Poland) for the lower part of the sedimentary record. However, four bulk sediment samples were excluded from the model (Table 1, Figure 2), since they show either younger or older ages that may have resulted from sediment reworking or introduction of old carbon into carbon-bearing deposits, leading to a reservoir effect that is common in lakes with long residence times (Cohen, 2003). Radiocarbon ages were calibrated using the IntCal20 calibration curve (Reimer et al., 2020) with online Calib 8.2 software (Stuiver & Reimer, 1993). The final age-depth model for Las Latas was performed using the R modelling package 'R-Bacon' using default settings for accumulation rate and memory parameters (Blaauw & Christen, 2011).

3.3 | X-ray diffraction analysis

The mineralogy of 117 samples from Las Latas core and 69 samples from Salina core was analysed by x-ray diffraction (XRD). Samples were selected based on lithofacies along the two cores. The Salina core sediments were subjected to a pre-wash due to the abundance of halite in the bulk sediment. The clay index was only used to normalise the percentage of the other mineral phases to 100%. The samples were dried for 24 h in an oven at 50°C and subsequently powdered in an agate mortar. Powdered samples were pressed into a pellet and measured using a Bruker-AXS D8 ADVANCE X-ray diffractometer DAVINCI design with a sample changer with a position sensitive detector (LYNXEYE XE-T) with 192 measuring points, using CuKα radiation ($\lambda = 1.5406$ Å) at 40 kV (Utrecht University, The Netherlands and at GEO3BCN-CSIC, Spain). Identification and semi-quantitative content of the mineral phases were obtained using Malvern Panalytical HighScore Plus software (Vrije Universiteit Amsterdam, The Netherlands) and using DIFFRACplus software (GEO3BCN-CSIC, Spain). Visual cross-checking confirmed consistent mineral phase identifications and relative peak intensities between the two datasets.

3.4 | Scanning electron microscopy and dispersive x-ray spectroscopy

SEM analyses were conducted on loose sediments to characterise the surface morphology of the carbonate grains. Samples were air-dried overnight and subsequently stub-mounted on adhesive carbon tape, and later sputter-coated with 10 nm Pt. They were then analysed using a Zeiss Gemini 450 equipped with an EDS detector (Utrecht University, The Netherlands).

3.5 | Stable carbon and oxygen isotope analyses

Stable carbon ($\delta^{13}C$) and oxygen ($\delta^{18}O$) isotopic analyses were conducted on 102 powdered bulk sediments obtained from Las Latas and Salina cores of LFP. Samples were pre-washed with Milli-Q water to remove sulphates. Their composition was measured from the released CO_2 after reaction with 100% H_3PO_4 under vacuum conditions, on a Finnigan MAT253 isotope ratio mass spectrometer (Thermo Scientific) using the Gasbench II preparation unit at the Vrije Universiteit Amsterdam, The Netherlands. The external reproducibility of the analyses was monitored by running the international standard IAEA-603 that yielded an average of 2.52‰ (SD = 0.06) for $\delta^{13}C$ and −2.35‰ (SD = 0.15) for $\delta^{18}O$.

TABLE 1 ^{14}C Age data for 'Las Latas' core. Four samples from the core '2013-04' in Laguna Fuente de Piedra are from Höbig et al. (2016). Radiocarbon dates excluded from the age model are indicated by *.

Number	Laboratory code	Core	Material	Depth (m)	Age ^{14}C yr BP ± 1σ	Age ^{14}C (cal yr BP)	2σ (cal yr BP)
1	COL2742.1.1	2013-04	Plant/wood	1.82–1.83	212 ± 53	190	426-0
2	COL2733.0.1	2013-04	Pollen	9.20–9.22	15,008 ± 226	18,335	18,818–17,781
3*	Las Latas 41-(B3-G)	Las Latas	Bulk sediment	10.58–10.59	33,700 ± 600	38,496	39,971–36,879
4	COL2729.0.1	2013-04	Pollen	11.44–11.55	19,159 ± 173	23,122	23,737–22,637
5*	Las Latas 49-(B3-O)	Las Latas	Bulk sediment	12.48–12.49	33,500 ± 600	38,277	39,722–36,674
6*	Las Latas 53-(B3-S)	Las Latas	Bulk sediment	13.38–13.39	37,200 ± 800	41,774	42,579–40,680
7	Beta-365747	2013-04	Bulk sediment	13.69–13.70	22,290 ± 100	26,674	26,965–26,336
8	Las Latas 69-(65)	Las Latas	Bulk sediment	18.08–18.09	28,810 ± 300	33,190	34,031–32,113
9	Las Latas 81-(77)	Las Latas	Bulk sediment	22.01–22.02	30,150 ± 350	34,610	35,315–34,034
10	Las Latas 98-(94)	Las Latas	Bulk sediment	30.38–30.39	36,500 ± 800	41,359	42,301–40,016
11*	Las Latas RC-33.6	Las Latas	Bulk sediment	33.65–33.66	29,740 ± 330	34,240	34,806–33,386
12	Las Latas 103b-(99b)	Las Latas	Bulk sediment	35.56–33.57	37,200 ± 1100	41,681	42,854–39,949
13	Las Latas 110-(106)	Las Latas	Bulk sediment	40.42–40.43	42,000 ± 2000	44,927	48,380–42,250
14	Las Latas RC- 45.87	Las Latas	Bulk sediment	45.86–45.87	43,000 ± 2200	45,829	50,090–42,392

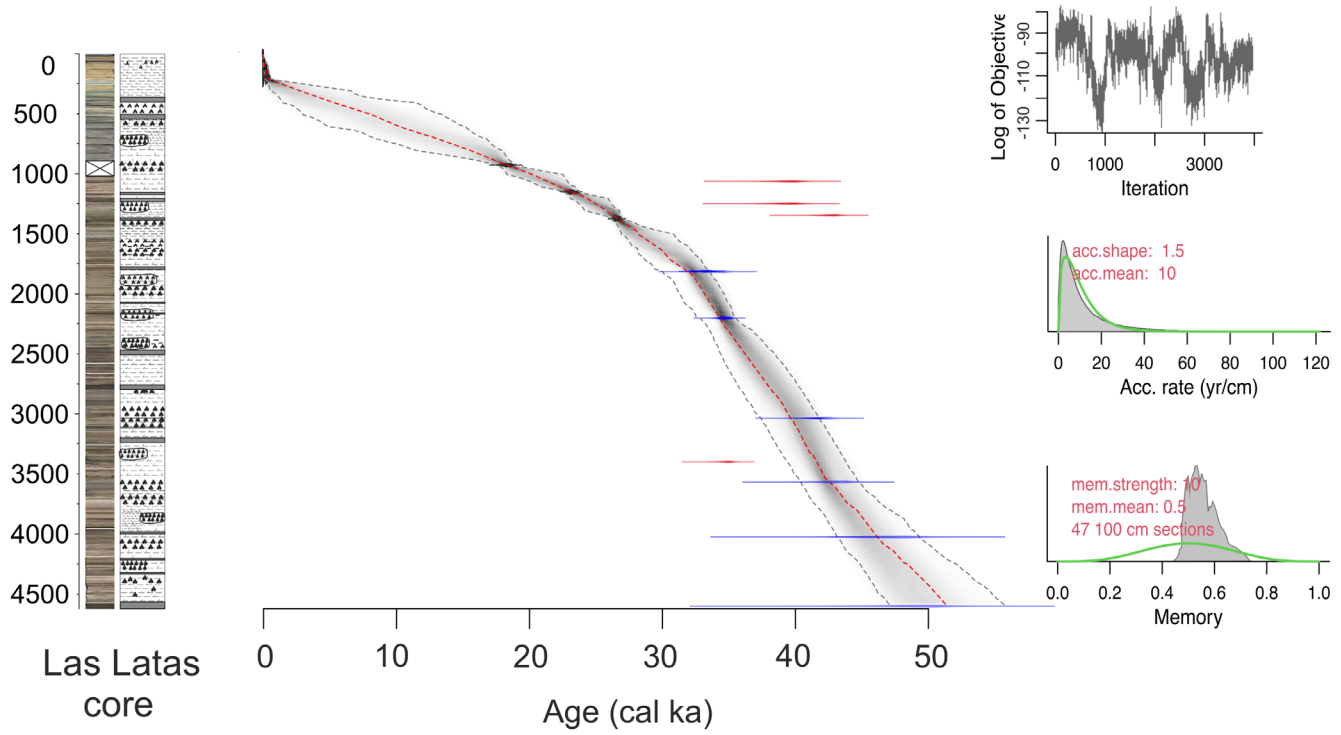

FIGURE 2 Age-depth model of the Las Latas sedimentary record, including graphs of MCMC iterations, distribution of the accumulation rate and memory. The grey area shows the range of iterations. Four data points from Höbig et al. (2016) are indicated in black, and six accepted age estimates from this study are indicated in blue. The excluded ages are indicated in red.

3.6 | Total organic carbon and nitrogen analysis

Total organic carbon (TOC) and nitrogen analysis was performed on powdered samples from both Las Latas and Salina cores, with sampling evenly distributed along core depth. Measurements were carried out using the Thermo Finnigan CNS Elemental Analyzer (FlashEA 1112) (Vrije Universiteit Amsterdam, The Netherlands). About 30 mg of loose sediment was weighed into silver capsules

and subjected to overnight fumigation with HCl (37%). Subsequently, 10 μL of 10% HCl was added to each sample and placed on a hot plate at 50°C until all the carbonate was removed. Samples were then dried and wrapped in tin capsules for further analysis.

3.7 | X-ray fluorescence core scanner analysis

The elemental compositions of the two sediment cores from LFP (Salina and Las Latas) were determined with the Avaatech XRF core scanner at the Royal Netherlands Institute for Sea Research (NIOZ), Texel, The Netherlands. The cores were scanned at 10 kV 'Mg-Fe' and 30 kV 'Mn-Rh' at 0.5 mA and 0.25 mA, respectively. The XRF analysis was performed on wet sediment with a 10 × 10 mm slit size and a detection time of 15 s per measurement. The core scanning was done with a 1-cm resolution. The sample was sealed with a 4-μm SPEXCerti Ultralene foil to reduce sediment dehydration and prevent contamination of the measurement prism during the analysis. For consistency control, eight pressed powder pellets of external reference standards were measured (GSR-4, GSR-6, GSD-10, JSd-1, JSd-3, MESS 3, SARM 2 and SARM 3). Line scan images were taken of the cores at F9.5 resolution.

3.8 | Pollen analysis

Twenty-one samples (~2 cm^3) from Las Latas core were picked from different depths and sedimentary facies to be processed for pollen analysis. Palynomorph extraction followed a modified version of Faegri and Iversen's methodology (Faegri et al., 1989). Pollen counting was performed under magnifications of ×400 and ×1000, with a minimum of 300 terrestrial pollen grains counted per sample. Fossil pollen was identified by comparing it to modern-day counterparts using published identification keys (Beug, 1961) and a modern pollen reference collection housed at the University of Granada, Spain.

Raw counts were converted into pollen percentages, excluding the aquatics (Cyperaceae, *Myriophyllum*, *Potamogeton* and *Typha*) from the terrestrial pollen sum, as these are often overrepresented in lacustrine environments and represent local vegetation. To differentiate between warm/humid phases (e.g. interglacial or interstadial) and cold/arid phases (e.g. glacial or stadial), a Pollen Climate Index (PCI) was calculated based on modern ecological inferences and calculated as Mediterranean tree taxa (including *Quercus*, *Olea*, *Pistacia* and *Betula*)/xerophytes (including *Artemisia, Ephedra and* Amaranthaceae). The percentage of *Artemisia* was also calculated, which has been previously shown to increase with cold and dry conditions in the region (Camuera et al., 2019).

4 | RESULTS

4.1 | Chronology

The chronology of Las Latas core is constrained by 10 radiocarbon ^{14}C ages (Table 1, Figure 2). The ages include bulk sediments, plant/wood and pollen. Four ages are incorporated from the core 2013-4 published by Höbig et al. (2016), and six new ages are derived from the Las Latas core of the current study. Together, these ages provide a chronological framework covering the time period from 52 to 0 cal ka. The age-depth model indicates that the sediment accumulation rate was not constant but rather shows a gradual decrease from the lower to the upper part of the core. Over the full sequence, the average accumulation rate is ~0.9 mm/year (Figure 2).

4.2 | Quaternary sedimentary sequence: Lithofacies in LFP

The core sediments are microcrystalline carbonates (aragonite, calcite, and dolomite) with sulphates (gypsum), silicates (clays and quartz) and halides (halite). Gypsum, along with halite, is commonly present in all carbonate facies, with contents ranging from 0% to 96.2% and 2.7% to 45%, respectively. According to the sedimentological and mineralogical characteristics, six distinct sedimentary facies dominate the lacustrine sequence of the two studied cores. A microscopic description of the core is presented (Figure 3).

4.2.1 | Calcitic mud (Facies I)

This facies consists of medium to thick beige beds ranging from 10 to 40 cm, composed predominantly of microcrystalline calcite, reaching up to 75% in Las Latas core and 62% in Salina core, with clays, quartz and gypsum. Diagenetic halite is common, represented by isolated crystals filling the porosity. Root traces are abundant throughout the interval. This facies is mainly found in the upper 210 cm of the Las Latas core and the upper 90 cm of the Salina core.

4.2.2 | Calcitic and aragonitic mud (Facies II)

This facies is represented by pale greenish to beige beds, ranging from 2 to 40 cm thick, microcrystalline calcite (up

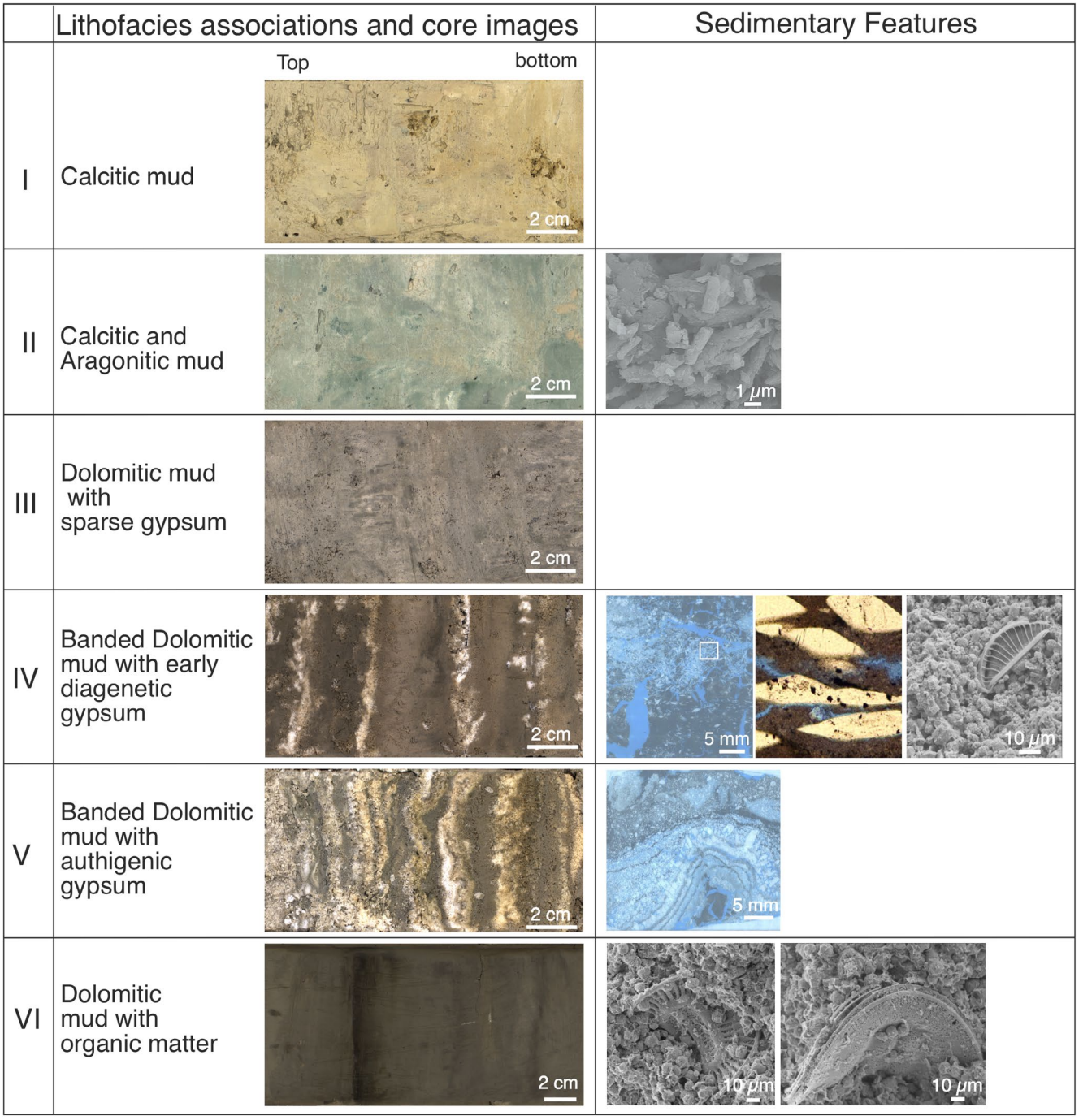

FIGURE 3 High-resolution images of the six main lithofacies associations (I–VI) and their sedimentary features comprising both sedimentary cores in Laguna Fuente de Piedra.

to 48%) and aragonite (up to 50%), with minor traces of dolomite. Microcrystalline gypsum occurs within the carbonate matrix. No distinct lamination is observed. This facies is restricted to the upper 6 m of the Las Latas core.

Dolomitic facies (III-IV-V-VI)

Dolomite dominates the carbonate facies, reaching up to 93% in both cores throughout the sequence. The following four facies are predominantly dolomitic with intercalated gypsum, differing mainly in their textural and diagenetic characteristics.

4.2.3 | Dolomitic mud with sparse gypsum (Facies III)

This facies is made of greyish brown beds of microcrystalline carbonates, composed mainly of dolomite with

varying proportions of calcite and/or aragonite (5%–39%). Gypsum occurs as sparse, scattered crystals within the carbonate matrix. The sediments are less compacted than the following facies. This facies occurs repeatedly in the upper 20.2 m of the Las Latas core and in variable layers along the Salina core. Lamination is not commonly significant, as it is disrupted by root marks.

4.2.4 | Banded dolomitic mud with early diagenetic gypsum (Facies IV)

This facies consists of brownish dolomitic mud layers intercalated with lenticular-shaped gypsum crystals. Lamination is less distinct compared to facies V. The lenticular gypsum crystals vary in size on the centimetre scale, reaching up to 2 cm. Additionally, diatom frustules are preserved within the carbonate mud.

4.2.5 | Banded dolomitic mud with authigenic gypsum (Facies V)

This facies consists of greyish-green dolomitic mud displaying well-defined lamination. Laminations are interspersed with microcrystalline gypsum crystals, some of them reaching up to 600 µm. The gypsum crystals are embedded in a carbonate matrix and exhibit no preferred orientation. Dolomite and gypsum laminae show microbial mat structures, with individual layers ranging from 2 to 3 mm in thickness.

4.2.6 | Dolomitic mud with organic matter (Facies VI)

This facies consists of dark grey to black layers of dolomitic mud with distinguished laminations, associated with microcrystalline gypsum. However, gypsum does not form significant layers. The total organic carbon (TOC) content in this facies is higher (up to 3%) compared to the other facies. Pelagic diatoms of uniform size are present along with well-preserved Characeae oospores.

4.3 | Phase morphology and structural characteristics

SEM images and EDS analysis of carbonate-rich sediments associated with other mineral assemblages (gypsum, halite) from LFP display the authigenic occurrence of dolomite (Figure 4). SEM observations show that dolomite aggregates in LFP appear as spherical structures embedded in an extracellular polymeric substance (EPS) matrix. In addition, dolomite crystals show cauliflower-shaped structures with associated bacterial voids in their centers and broken bacterial cells (Figure 4B,C).

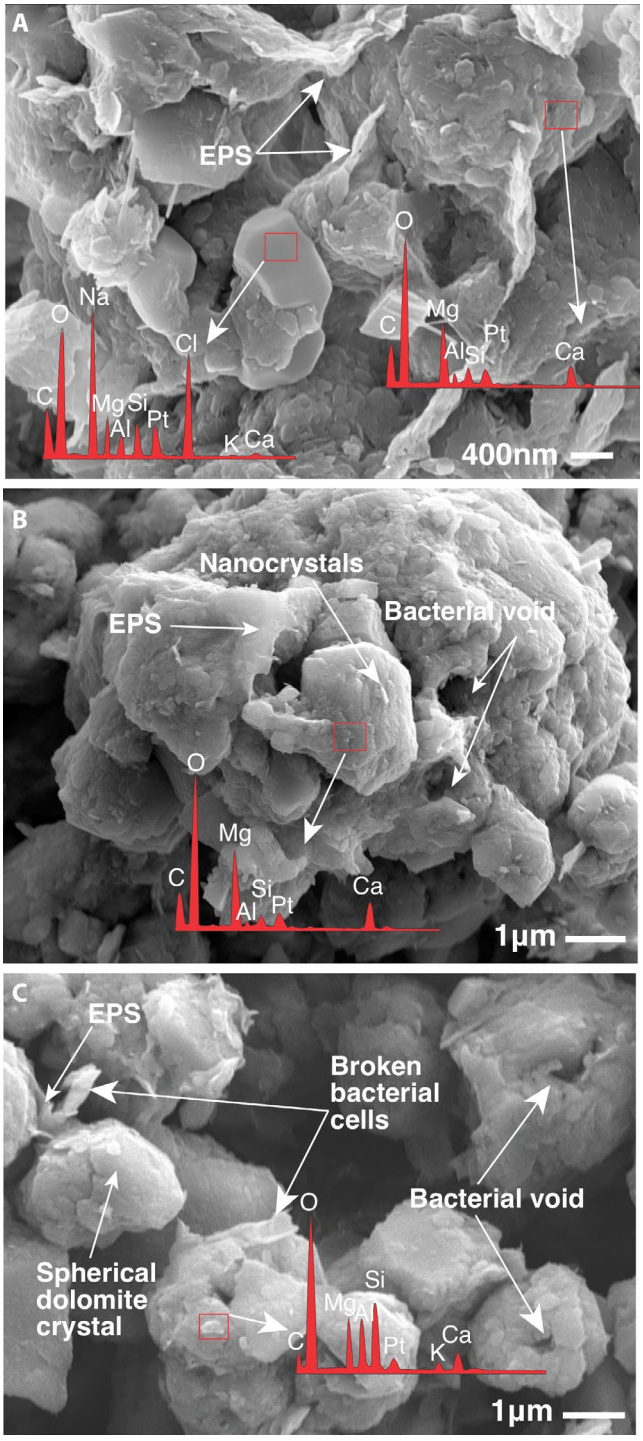

FIGURE 4 SEM images with EDS spectra of samples from Laguna Fuente de Piedra. (A) Microcrystalline, spherical-shaped dolomite crystals along with other minerals embedded in extracellular polymeric substance (EPS). Images (B) and (C) highlight broken bacterial cells, in addition to dolomite grains composed of nanocrystals with central voids, which can be indicative of bacterial voids.

4.4 | Geochemistry

4.4.1 | Stable isotopic composition ($\delta^{18}O$ and $\delta^{13}C$) of carbonates

The values $\delta^{18}O$ and $\delta^{13}C$ in total bulk carbonate of the sediment samples are represented in (Figure 5A,B) and listed in Tables S1 and S2. Samples with mixed carbonates in the upper ~6 meters in the Las Latas core show $\delta^{18}O$ values ranging between −0.57‰ and 2.33‰ and $\delta^{13}C$ values ranging between −4.49‰ and −2.05‰. With depth, $\delta^{13}C$ values of dolomite vary in range from −6.58‰ to −3.30‰ and $\delta^{18}O$ values from 3.16‰ to 5.64‰.

Dolomite samples in the lake are more enriched in $\delta^{18}O$ and have a tendency to be more depleted $\delta^{13}C$ values compared to the mixed carbonate samples. This variation is visible in the stratigraphic profile (Figure 5A,B), which shows a general trend of increasing $\delta^{18}O$ and decreasing $\delta^{13}C$ values with depth.

4.4.2 | Total organic carbon (TOC) and carbon to nitrogen ratio (C/N)

LFP sediments record low TOC values reaching up to 3.0% in the Las Latas core and only up to 1.6% in the Salina core (Tables S1 and S2). This can be observed along the stratigraphic profiles (Figure 5A,B). The C/N ratio exhibits isolated high values, reaching up to ~80 in a few samples from the Las Latas core with no significant trend. Contrary to the latter, the C/N ratio in the Salina core depicts a decreasing trend towards the top of the core.

4.4.3 | X-ray fluorescence analyses (XRF)

XRF data from the two sedimentary cores show variations in elemental composition throughout the sequence (Figure 6A,B). Magnesium (Mg) content shows a slight decrease towards the top of the cores, whereas the potassium to silicon ratio (K/Si), along with aluminium (Al) and iron (Fe), depicts an increase towards the top of the core. Evaporative conditions in the lake are inferred from calcium to titanium ratios [log(Ca/Ti)] and sulphur (S) trends. The Ca/Ti ratio serves as a geochemical indicator of calcium enrichment linked to in-lake mechanisms, such as evaporation or biological activity (Brown et al., 2007; Davies et al., 2015). Log(Ca/Ti) demonstrates a positive correlation with sulphate layers throughout both sedimentary cores, with a decrease towards the top where gypsum becomes less abundant in the record. Sulphur, indicative of the sulphate layers in the cores, shows a consistent decreasing trend upwards in the Las Latas core. Meanwhile, the Salina core displays a less pronounced trend, with sulphur peaks occurring in variable distribution. Within facies VI, distinct high sulphur peaks occur in certain layers.

4.5 | Palynology

To have a general insight into the vegetation and the climatic trends, pollen analysis was carried out. The analysis was done as a preliminary approach by processing 21 samples from different depths and sedimentary facies in the Las Latas core. Figure 5A shows a general increasing trend in *Artemisia* from 1.27% up to 26.9% before 39 cal ka, which is reflected in the gradual decrease of the PCI from 8.25% to 0.03%. This is followed by a gradual drop and a maintenance of generally low values of Artemisia to 1.25%, with an increase in PCI to 5.2% at almost 30 cal ka, which will be further explained below. During the shorter period between ~30 and 24.7 cal ka, *Artemisia* increases, reaching its maximum at 27.3% while PCI decreases, reaching 0.3%. This is followed by the gradual decrease of Artemisia starting at the onset of the Holocene, with some minor increasing events until reaching a value of 8.8%.

5 | DISCUSSION

Playa lake deposits in closed basins are valuable archives for past climatic shifts. Even minor fluctuations in evaporation or precipitation led to substantial changes in lake water levels and salinity in closed-basin lakes (Battarbee, 2000). These changes are reflected in the studied cores, where variations in lithology and geochemistry suggest dynamic hydrological and geochemical conditions. Additionally, variations in organic matter in sediments are influenced by paleoclimatic changes (Meyers & Lallier-Vergès, 1999; Ortiz et al., 2010) and serve as indicators of paleoproductivity (Meyers, 1997).

5.1 | Carbonate dynamics in the playa lake system

LFP shares characteristics commonly associated with an actively evolving continental sabkha, where prolonged aridity periods are interrupted by episodic flooding, favouring shifts in water levels that affect sedimentation. The presence of minerals such as dolomite and gypsum, along with evidence of repeated phases of water influx reflected by enhanced detrital input and desiccation, suggests that conditions similar to those found in

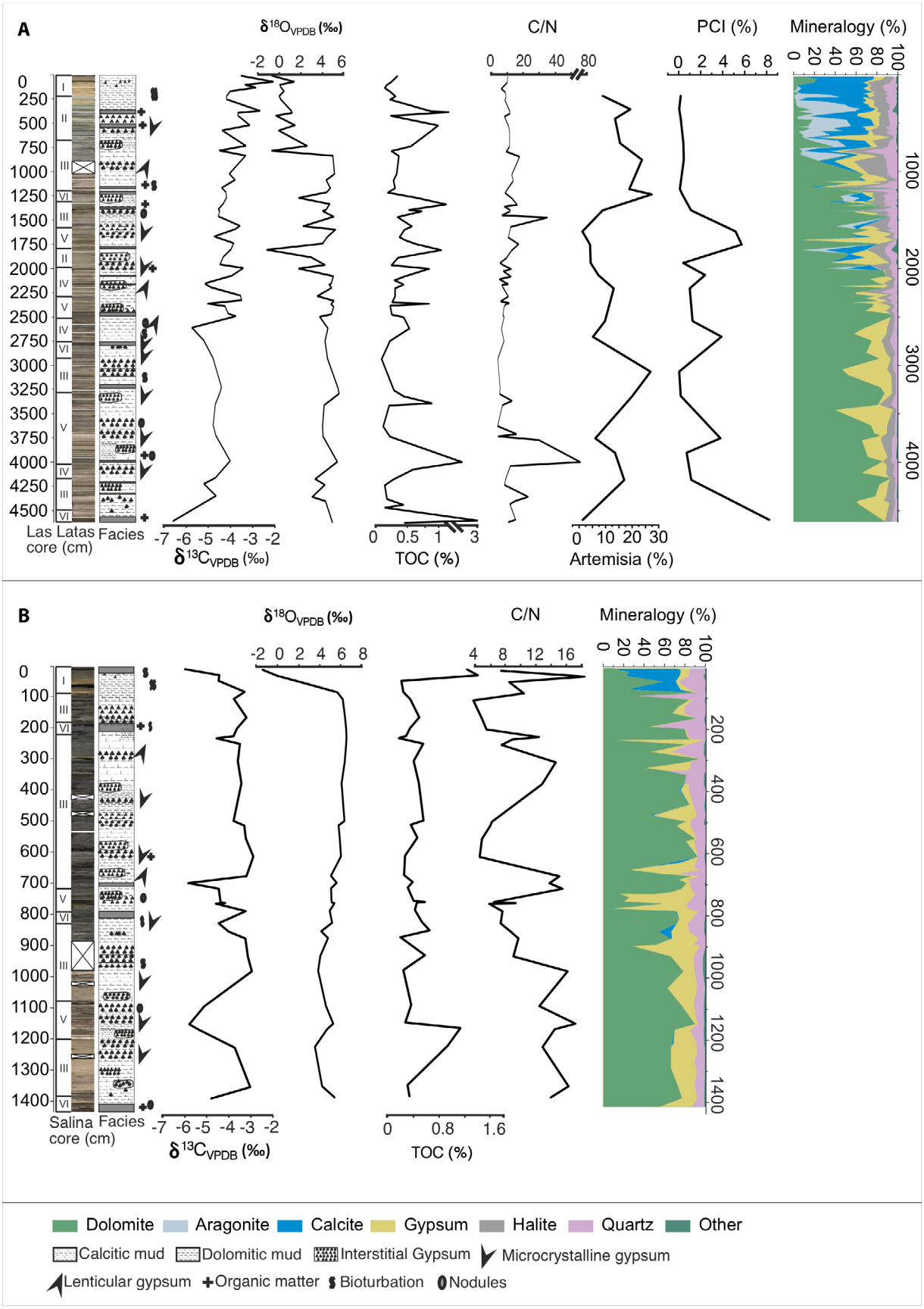

FIGURE 5 Stratigraphic column of (A) 46.2-meter-long Las Latas core and (B) 14.4-meter-long Salina core in Laguna Fuente de Piedra, with the different lithofacies, mineral distribution, isotopic composition ($\delta^{13}C$), ($\delta^{18}O$), total organic carbon (TOC), C/N ratio and pollen content with depth.

continental sabkha environments occurred at certain times. This aligns with the idea that different lacustrine hydrology systems lead to continental sabkhas being widespread in ephemeral lake systems (Warren, 2016). However, the variability in facies succession and mineral precipitation in the studied cores indicates that the system did not remain fixed but instead responded dynamically to climatic and tectonic changes, with shifts in water chemistry controlling carbonate and sulphate precipitation. This is supported by the findings of Jiménez-Bonilla et al. (2024), who concluded that the Las Latas and La Nava faults, which were active during the Quaternary, led to the migration of the lacustrine basin and controlled its sedimentation over time.

Carbonate sedimentation is constrained by several factors, including alkalinity, pH, salinity, temperature, redox conditions, and organic productivity of the basin (Gierlowski-Kordesch, 2010; Last, 1990; Mackenzie et al., 1983). These physicochemical conditions are, in turn, influenced by the lake's water balance and regional climate. While XRF trends might generally indicate the abundance of dolomite compared to other carbonate facies, the high Mg concentration in the groundwater of LFP suggests an alternative explanation. Mg is likely incorporated into Mg-rich clays associated with the carbonates. Therefore, there is no significant correlation between Mg concentrations and the dolomite abundance throughout the record (Figure 6A,B).

In the deeper intervals of both the Las Latas and Salina cores, dolomitic mud lithofacies (III, IV, V, VI) reflect the different episodes of dolomite precipitation within the lake. Generally, the $\delta^{18}O$ values in these sediments, which are higher than those in facies I and II, indicate conditions of intense evaporation with limited water influx, suggesting that dolomite precipitation occurred under drier conditions. The stratigraphic profiles show the recurrence of facies, which suggests episodic changes in water availability and chemistry in response to fluctuations in evaporitic conditions over time. For example, facies V features dolomite interlayered with primary microcrystalline gypsum in well-defined laminations. These thin laminations that alternate between sulphates and dolomite align with the annual and inter-annual oscillations previously observed in the water budget of the lake (Rodríguez-Rodríguez et al., 2016b).

Furthermore, the high dolomite content, without a corresponding increase in quartz or clay fractions, points to an authigenic origin for the dolomite. This is supported by SEM images (Figure 4), which reveal the preservation of microbial compounds (EPS, bacterial voids, broken bacterial cells) within the dolomite crystal structure at the nanometric scale. As described in Section 4, the dolomite aggregates exhibit spherical structures embedded in an EPS matrix, which enhances the formation of dolomite by providing nucleation sites for its precipitation (Bontognali et al., 2014; Sánchez-Román et al., 2008, 2011a, 2011b, 2025; Vasconcelos & McKenzie, 1997). These observations are consistent with recent advances in the understanding of dolomite formation in shallow saline environments. Dolomite has traditionally been considered a diagenetic mineral due to the lack of evidence for direct inorganic precipitation at low temperature and pressure, even in saturated solutions (Land, 1998). However, over the last three decades, significant advances have been made in the understanding of dolomite formation, particularly the role of microbial processes in facilitating its precipitation. Various saline, shallow environments were shown to produce dolomite with the help of bacteria, which facilitate the specific physicochemical conditions required for its precipitation within EPS-rich environments (Bontognali et al., 2008; Sánchez-Román et al., 2008, 2009a). Examples of this process were documented in several modern analogues, such as the Coorong Lakes in Australia (Wright, 1999), Lagoa Vermelha in Brazil (Vasconcelos & McKenzie, 1997), and sabkha systems of the Persian Gulf (Sadooni et al., 2010; DiLoreto et al., 2019). LFP represents a well-characterised shallow continental sedimentary setting, where dolomite is the dominant carbonate phase in several stratigraphic intervals and accumulates at high sedimentation rates. The facies richest in dolomite (Facies III-VI) are associated with extreme aridity and commonly co-occur with gypsum crystals, resembling sabkha-like settings. In contrast, facies linked to wetter periods (Facies I and II), characterised by ephemeral lake conditions, contain lower percentages of dolomite. This facies distribution highlights the potential for saline, shallow environments in arid regions to function as dolomite 'factories', with sedimentation rates potentially comparable to those observed in marine calcite-producing settings.

Moving upwards in the studied core records, mineralogical profiles of the Las Latas and Salina cores reveal a major event characterised by an abrupt shift in carbonate facies. In the upper section (I and II) of the Las Latas sedimentary core, there is a transition to a dominance of calcite and aragonite, while the Salina core shows a predominance of only calcite (Figure 5A,B). This shift is accompanied by a decrease in gypsum and an increase in quartz, indicating an increase in detrital input. These changes suggest significant flooding events, indicating increased water availability and a relatively stable hydrological balance. Similar depositional episodes were documented in regional playa lakes, where calcite is prevalent in the upper (i.e. younger) sections of the cores (e.g. Gil-Márquez et al., 2022; Giralt et al., 1999; Martín-Puertas et al., 2009; Pérez et al., 2002; Queralt et al., 1997; Valero-Garcés et al., 2000, 2006). Additionally, the absence of lamination in these upper depositional layers

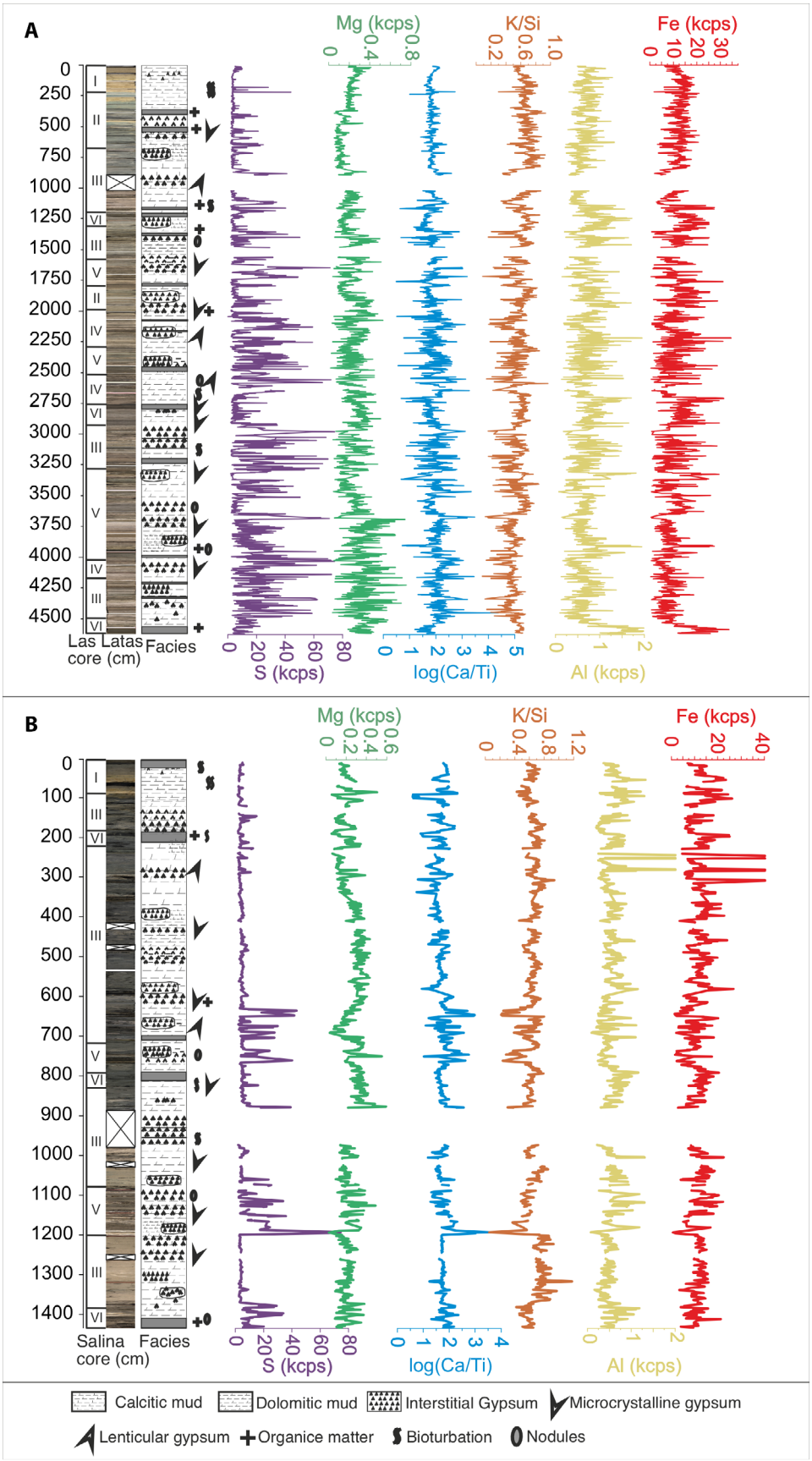

FIGURE 6 Stratigraphic column and associated lithofacies, along with geochemical profiles from XRF dataset, presenting relations between different elements and elemental ratios along (A) 46.2-meter-long Las Latas core and (B)14.4-meter-long Salina core.

suggests bioturbation under sustained oxic conditions in the water column (Valero-Garcés et al., 2003). The carbonate sediments, predominantly calcite and aragonite, exhibit $\delta^{13}C$ values reaching −2‰. Facies I and II demonstrate lower $\delta^{18}O$ values than other facies, indicating warmer and more humid conditions.

The absence of aragonite in the upper part of the Salina core in LFP, where dolomite is present instead, suggests that the mid-eastern depocentre experienced chemical conditions that did not favour aragonite precipitation. Unlike the marginal zone (Las Latas core), where aragonite and calcite accumulated in the upper 6 meters, the depocenter (Salina core) likely retained water for longer periods due to slower desiccation (Figure 7). A shift towards wetter conditions during the Holocene decreased the salinity in the playa lake, inhibiting microbial precipitation of dolomite during the humid periods and thus favouring the precipitation of the other carbonate phases. However, during periods of partial desiccation, the lake water may have evolved into a brine that was retained in the depocenter at the Salina core site. Sánchez-Román et al. (2009b) reevaluated the traditional view that sulphate inhibits dolomite precipitation, demonstrating that in the presence of sulphate-reducing bacteria (SRB), dolomite can still form at low temperatures. If sulphate reduction was active in Salina, as it has been inferred to be an active mechanism in LFP (Höbig et al., 2016), it likely altered carbonate equilibria by increasing alkalinity and modifying porewater chemistry, thereby favouring dolomite precipitation over aragonite. In addition, the presence of organic compounds (e.g., EPS, broken bacterial cells; Figure 4) probably facilitated this process by creating localised viscous microenvironments that enhanced dolomite nucleation (Sánchez-Román et al., 2011a). The resulting increase in salinity in that part of the playa lake created similar conditions to those during the earlier periods of dolomite formation in the Las Latas site, plausibly explaining why dolomite preferentially precipitated under these circumstances in Salina. The difference in mineralogical evolution between the two cores highlights variations in lake hydrology and geochemistry, indicating how depositional setting controls carbonate precipitation pathways in playa lake systems.

5.2 | Paleoclimatic reconstruction

The sedimentary records of LFP provide a multi-proxy, paleoenvironmental investigation, offering valuable insights into local and regional climatic trends, including episodes of aridity and humidity. Based on age estimates from the Las Latas core, the 46.2 m sedimentary sequence in LFP is inferred to extend back to the Late Pleistocene. As reported by Höbig et al. (2016), establishing chronological control in LFP is challenging due to the very low plant organic content in the lake's core sediments and the lake's highly dynamic response to regional environmental and climatic shifts. Despite the constraints imposed on the

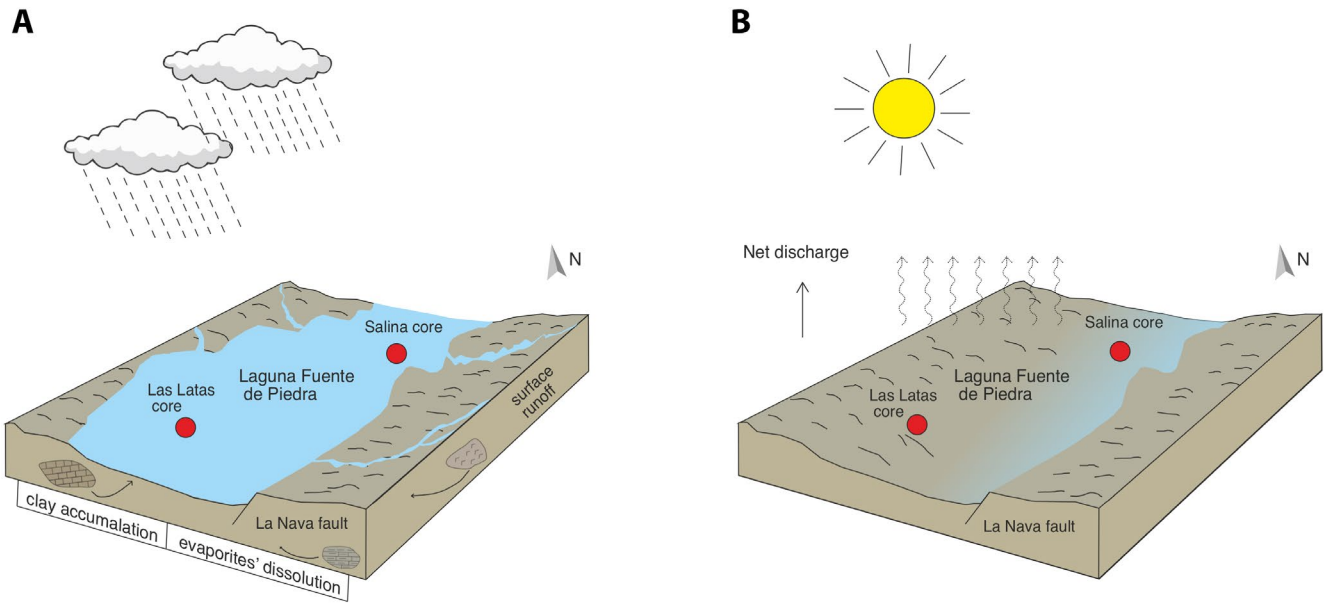

FIGURE 7 Conceptual model of Laguna Fuente de Piedra illustrating the depositional processes during wet and dry periods in the closed basin. (A) Wetter periods characterised by increased surface runoff, groundwater circulation and dissolution of pre-existing evaporites, with physicochemical conditions favourable for calcite and aragonite accumulation. (B) Dry conditions promoting dolomite and gypsum precipitation, with varying desiccation periods in the lake controlled by tectonic activity, influencing the water retention time and the local geochemical conditions. Red dots show the Las Latas and Salina core sites.

pollen data by their low resolution, they can still provide insights into the general environmental trends affecting the lake throughout its evolution. Previous paleoclimate studies of Mediterranean sites have indicated the influence of Atlantic and Mediterranean climate oscillations on the Iberian Peninsula (Camuera et al., 2022; González-Sampériz et al., 2006).

5.2.1 | Late Pleistocene

Lake sedimentary sequences in the Iberian Peninsula, which cover the last glacial period in the Pleistocene epoch and display responses to dry and wet climatic shifts, are weakly reported in comparison to marine records. This likely reflects the difficulties in establishing accurate chronological records in lake sediments that could limit the study of these climatic fluctuations.

The XRF data and the detailed images reported here provide a better resolution than the XRD data in terms of overviewing the sulphate layers, implying the formation of evaporite layers in annual cycles during the last two stages of the last glacial period. To better understand the climatic patterns represented in the Las Latas sequence, two paleoclimatic records from southern Spain are used for comparison: Alboran Sea surface temperature (SST) data for tracking past temperature fluctuations in southern Spain (Martrat et al., 2004) and mean annual precipitation (MAP) reconstruction in Laguna de Padul for identifying precipitation patterns across the southern Iberian Peninsula (Camuera et al., 2022). The sulphur counts in the studied core indicate periods of extensive evaporite minerals precipitation, primarily observed in the lower part of the Las Latas core (Figure 8). These data show a slight negative correlation between sulphur counts and both SST and MAP, suggesting that gypsum deposition peaked during colder, drier periods of the last glacial. The reconstruction reveals several abrupt stadial-interstadial shifts during the last glacial period, characterised by geochemical shifts and sedimentary facies changes. These shifts may correspond to Dansgaard–Oeschger (DO) cycles, which are repeated series of abrupt millennial scale climate warming events identified in Greenland ice core records (Dansgaard et al., 1984), as well as Heinrich events, which are extreme iceberg discharge episodes documented in North Atlantic deep marine sediment cores (Heinrich, 1988).

During Marine Isotope Stages (MIS) 3 and 2, clear shifts in climatic conditions are noted in the Las Latas record. A clear transition to an arid phase is marked by an increase in $\delta^{18}O$ at around 46.5 cal ka, with a visible sedimentary change from Facies IV to V that depicts clear gypsum laminations. The PCI, which was applied in various studies to distinguish between alterations in cold–dry and warm–wet phases based on the ratio of thermic to steppic taxa (Camuera et al., 2019, 2021; Jiménez-Moreno et al., 2023; Joannin et al., 2011), shows a decreasing trend during this period, suggesting cold and dry conditions during the Late Pleistocene. Such an event in the western Mediterranean, mainly in the Abric Romaní sequence, was subsequently associated with HE5 due to the cold-phase aridity peaks by Burjachs et al. (2012). In south-east Spain, the cold-dry event identified at ~46.5 cal ka in the Las Latas record can likewise be associated with HE5, for which LFP exists.

After the cold-dry event at ~46.5 cal ka, several proxies in the Las Latas record indicate continuous climatic fluctuations between wet and dry episodes. These include distinct sulphur peaks, which suggest seasonal evaporite precipitation during the periods of desiccation, while wetter conditions favoured dolomite precipitation while water was still present. In addition, significant changes in carbonate mineralogy are observed, marked by episodes of calcite and aragonite precipitation in the lake along with dolomite between 12.5 m and 20 m depths, corresponding to an approximate time range of ~33 and 25 cal ka. Taking into account the uncertainties associated with our age model, HE3 is likely linked to the sharp decrease in $\delta^{18}O$ between approximately 29 cal ka, corresponding to a change in lithofacies from V to III, representing a distinct interruption of a dry climatic stage resulting in a noticeable increase in moisture. In addition, this phase shows a decline in *Artemisia* to 1.25%, indicating more humid but still cold conditions during this event. This interpretation is also supported by the simultaneous drop in sulphur content, indicating the absence of evaporite precipitation during this interval, consistent with wetter conditions. This correspondence to a moist period in southeastern Spain is also indicated by Camuera et al. (2022) in the Padul record, in which the MAP reconstruction shows higher values in that period in comparison with the dry periods.

As the Las Latas sequence shows different climatic responses to Heinrich events, it is suggested that the HE2 event occurs approximately between ~24.8 and 23.5 cal ka (depth interval 11.5–12.3 m), characterised by cold and arid conditions. This period is marked by low organic productivity, indicated by decreased TOC values, low lake levels reflected by the high presence of evaporitic layers, and reduced detrital input as shown by low Fe, Al, and K/Si values. Additionally, an increase in $\delta^{18}O$ values suggests enhanced evaporation, consistent with the given arid conditions (Figure 5A).

During HE2, the pollen record from the Las Latas sequence is characterised by low PCI values ranging between 0.1% and 0.3%, indicating cold and dry conditions.

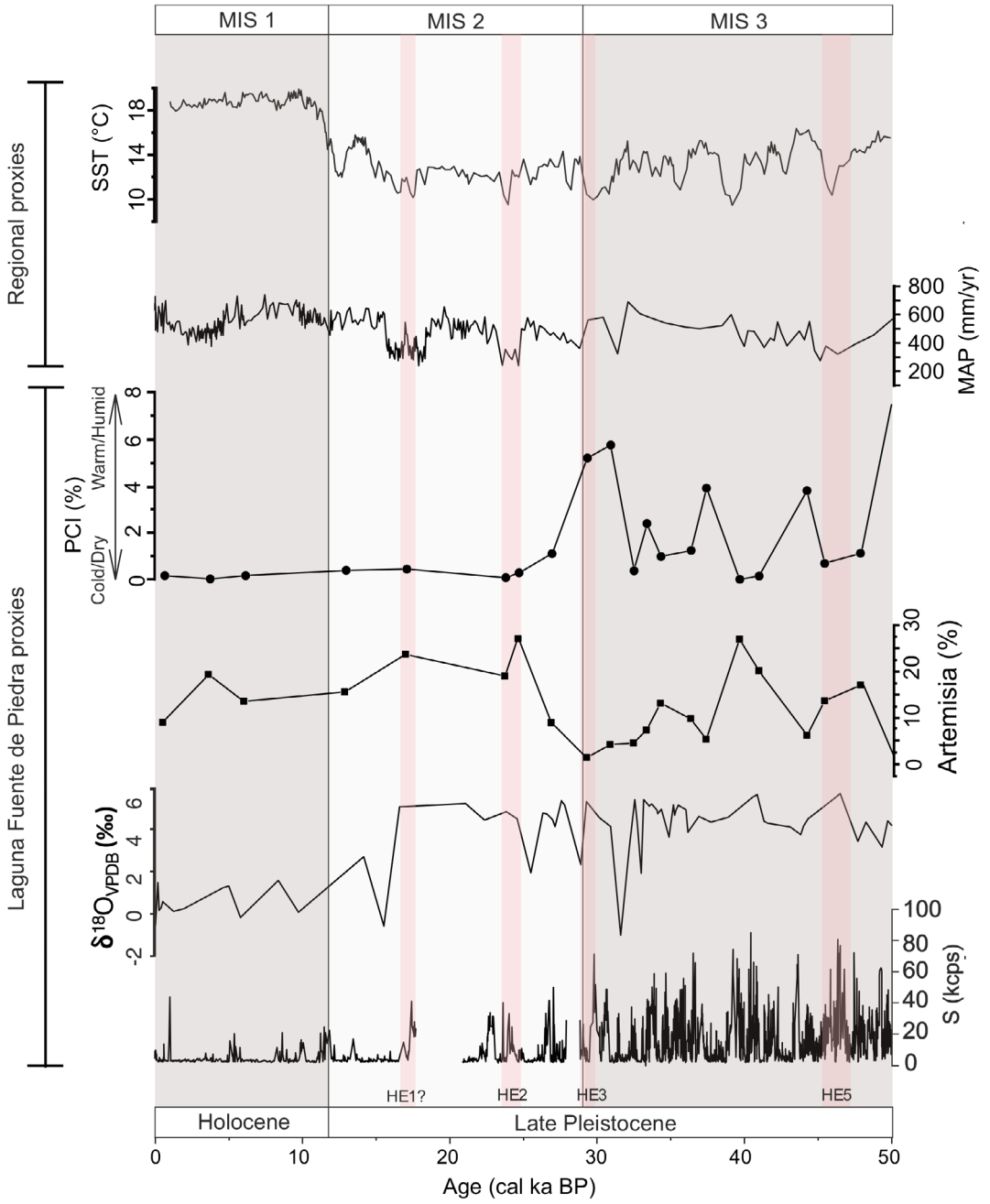

FIGURE 8 Correlation between local proxies from the Las Latas record in Laguna Fuente de Piedra (sulphur counts, $\delta^{18}O$ values, pollen data) and regional paleoclimate proxies, including mean annual precipitation (MAP) of the Laguna de Padul record (Camuera et al., 2022) and sea surface temperature (SST) of the Alboran Sea record (Martrat et al., 2004). Marine Isotope Stages (MIS 1–3) are shown along with potential intervals of Heinrich events (HE1-HE5) based on patterns observed in Las Latas record.

These patterns in HE2 are similar to previously reported findings from central Spain (Fuentillejo maar-lake; Vegas et al., 2010) and northeastern Spain (El Portalet peatbog; González-Sampériz et al., 2006), highlighting a consistent regional climatic response during this period. In addition, the dominance of *Artemisia*, which reaches a maximum of 27.3% in the pollen record, points to an expansion of steppe and semi-desert vegetation. The geochemical data with the associated vegetation assemblages indicate lake drainage and desiccation during the period corresponding to HE2.

Following HE2, sediment was partially recovered within a timeframe that complicates the establishment of a precise chronology for the last glacial maximum (LGM), which may have occurred during this period. The lithofacies were most likely deposited under generally cold and arid conditions, characterised by seasonal scale climatic oscillations, persisting until the transition into the

Holocene between 23.5 and 11.7 cal ka. This cold and arid phase aligns closely with the significant cold events recorded in the Alboran SST dataset, which could include both the HE1 and Young Dryas events. TOC values remain consistently low, with $\delta^{18}O$ values staying relatively high, accompanied by the continuous enrichment of *Artemisia* and a marked depletion in PCI values.

Within this cold-arid period, a significant change in mineralogy is observed between ~16 and 14.2 cal ka, characterised by an increase in aragonite and calcite and a decrease in dolomite to ~5%. Quartz input also increases up to ~33%. The onset of this shift is marked by a sharp decrease in $\delta^{18}O$ values to −0.57‰. Together, these opposing signals relative to the cold-arid conditions suggest a warmer and wetter climate compared to the preceding events and likely correspond to an early regional onset of Bölling–Allerød (B–A) interstadial. The hydrological conditions of LFP during the B–A interstadial were most likely controlled by groundwater, which provided a continuous water supply throughout this humid period. Previous regional pollen records show a forest development during the B-A, associated with climatic conditions such as temperature and precipitation similar to those observed during the Holocene (Fletcher et al., 2010).

5.2.2 | Holocene

Following the Younger Dryas, the transition into the present interglacial Holocene that began at approximately 11.7 cal ka is distinguished by a relatively more stable climate in comparison to the Pleistocene.

Generally, previously reported data from regional lakes like Laguna de Salines (Burjachs et al., 2016), Laguna Seca (Jiménez-Moreno et al., 2023; López-Avilés et al., 2022) suggest that hypersaline conditions after the end of the Younger Dryas (11.7 cal ka) likely persisted before transitioning to increasingly wetter conditions. In LFP, the presence of thick laminated gypsum layers, interbedded with thin carbonate-rich mud (facies IV and V), indicates environmental conditions similar to those observed in other regional lakes up until almost 11.3 cal ka, in which dry conditions persisted before the transition into a moist phase. This implies that the lake water level likely remained low throughout the Younger Dryas–Holocene transition.

Following the period between ~11.7 and 11.3 cal ka, the sedimentary facies show a reduced persistence of lamination and a mixture of dark green to grey mud that is attributed to seasonal flows from runoffs and streams, which transported detrital input into the lake catchment, causing rapid sediment accumulation during that period. This is further supported by an increase in K/Si ratios in this interval (Figure 6A), indicating enhanced clay influx under wetter conditions. A positive correlation between K and clay abundance, with its association to an increasing detrital input, was reported in similar lake systems (Moreno et al., 2011; Ramos-Román et al., 2018). The scarce occurrence of gypsum further suggests high lake water levels, as rising water levels would inhibit evaporite deposition. This period was also distinguished by a slight increase in TOC values that are associated with the preservation of organic matter and siliciclastic elements, indicating moist conditions. As mentioned previously, Camuera et al. (2022) provided a quantitative reconstruction of the MAP in Lake Padul, the oldest southernmost continental archive in the Iberian Peninsula (range of 200 cal ka), reflecting precipitation variations in southern Spain. Their dataset reveals a significant increase in MAP from the early Holocene onwards, which correlates with the deposition of calcite and aragonite layers in LFP. Formation of evaporites in the lake significantly decreased in this epoch (Figure 8).

6 | CONCLUSIONS

Results suggest that LFP serves as a significant archive for paleoclimatic and paleoenvironmental changes in the western Mediterranean over the past ~50,000 years. The application of multi-proxy analysis, integrating geochemical and mineral-lithological data, has provided valuable insights into the processes influencing saline playa lake catchments.

The evaporite-dolomite associations identified in the Salina and Las Latas sedimentary cores offer a robust proxy record of past hydrological and climatic conditions, contributing to our understanding of Quaternary climate dynamics in arid and semi-arid regions. This interpretation is further supported by the dominance of dolomite in the lower part of the cores, reflecting precipitation during the Pleistocene, while aragonite and calcite become more abundant in the upper sections. Their occurrence is most prominent during the Pleistocene–Holocene transition and extends into the Holocene. The authigenic formation of dolomite, mediated by microbial processes, highlights a key interface between biological and geochemical factors in the system balance.

Transitions between dry and wet phases are represented by six major sedimentary facies, each one reflecting specific environmental conditions. These facies range from calcitic and aragonitic mud to dolomitic muds with varying gypsum content. The transitions in facies indicate significant climatic shifts that influenced the deposition of both carbonates and evaporites in the lake. Drier and colder periods caused higher evaporative conditions, resulting in the

formation of gypsum–dolomite couplets. These phases also correspond to lower lake water levels. Wetter periods, on the other hand, were marked by higher clastic input and the precipitation of calcite–aragonite facies, associated with a higher water table in the lake. Finally, the depositional history of LFP suggests that it does not represent a stable setting but rather transitions between a playa lake and a continental sabkha depending on the tectonic activity and prevailing climate conditions. This study contributes to paleoclimatic reconstruction in the Iberian Peninsula and enhances our understanding of the factors driving carbonate precipitation in semi-arid environments.

ACKNOWLEDGEMENTS

This research was funded by the Dutch Research Council (NWO), Project Nr.: OCENW.KLEIN.037. MSR also acknowledges financial support from the Beatriz Galindo Senior Grant No. BG23-00132. We would like to express our gratitude to Suzan Verdegaal-Warmerdam for her invaluable assistance with stable C and O isotope analysis, and to Martine Hagen for her support with CN elemental analysis. Piet van Gaever is acknowledged for his assistance with XRF analyses at NIOZ and Willem Blom for his contributions to the development of the age model. Finally, we acknowledge the former director of Laguna de Fuente de Piedra, Manuel Rendón Martos, and the current director, África Lupión, as well as the Delegación Territorial de Desarrollo Sostenible en Málaga of Junta de Andalucia (Spain) for granting access to the lake and facilitating the initiation of the drilling campaign. Additionally, we acknowledge the contributions of Javier Jaimez Ávila from Centro de Instrumentación Científica (Spain), whose efforts in operating the drilling equipment and core recovery were essential in the success of this study. We thank the editor in chief, associate editor, and two anonymous reviewers for their time and constructive feedback, which helped improve the quality of this manuscript.

CONFLICT OF INTEREST STATEMENT

The authors declare no conflict of interest.

DATA AVAILABILITY STATEMENT

The data that support the findings of this study are available from the corresponding author upon request.

ORCID

Zeina Naim https://orcid.org/0009-0001-2868-4884

REFERENCES

Battarbee, R.W. (2000) Palaeolimnological approaches to climate change, with special regard to the biological record. *Quaternary Science Reviews*, 19(1–5), 107–124.

Beug, H.-J. (1961) *Leitfaden der Pollenbestimmung für Mitteleuropa und angrenzende Gebiete*. Stuttgart: Gustav Fischer Verlag.

Blaauw, M. & Christen, J.A. (2011) Flexible paleoclimate age-depth models using an autoregressive gamma process. *Bayesian Analysis*, 6(3), 457–474.

Bontognali, T.R., McKenzie, J.A., Warthmann, R.J. & Vasconcelos, C. (2014) Microbially influenced formation of Mg-calcite and Ca-dolomite in the presence of exopolymeric substances produced by sulphate-reducing bacteria. *Terra Nova*, 26(1), 72–77.

Bontognali, T.R., Vasconcelos, C., Warthmann, R.J., Dupraz, C., Bernasconi, S.M. & McKenzie, J.A. (2008) Microbes produce nanobacteria-like structures, avoiding cell entombment. *Geology*, 36(8), 663–666.

Brown, E., Johnson, T., Scholz, C., Cohen, A. & King, J. (2007) Abrupt change in tropical African climate linked to the bipolar seesaw over the past 55,000 years. *Geophysical Research Letters*, 34(20), 2007GL031240.

Burjachs, F., Jones, S.E., Giralt, S. & de Pablo, J.F.-L. (2016) Lateglacial to Early Holocene recursive aridity events in the SE Mediterranean Iberian Peninsula: The Salines playa lake case study. *Quaternary International*, 403, 187–200.

Burjachs, F., López-García, J.M., Allué, E., Blain, H.-A., Rivals, F., Bennàsar, M. & Expósito, I. (2012) Palaeoecology of Neanderthals during Dansgaard–Oeschger cycles in north-eastern Iberia (Abric Romaní): from regional to global scale. *Quaternary International*, 247, 26–37.

Calaforra, J.M. & Pulido-Bosch, A. (1999) Gypsum karst features as evidence of diapiric processes in the Betic Cordillera, Southern Spain. *Geomorphology*, 29(3–4), 251–264.

Camuera, J., Jiménez-Moreno, G., Ramos-Román, M.J., García-Alix, A., Jiménez-Espejo, F.J., Toney, J.L. & Anderson, R.S. (2021) Chronological control and centennial-scale climatic subdivisions of the Last Glacial Termination in the western Mediterranean region. *Quaternary Science Reviews*, 255, 106814.

Camuera, J., Jiménez-Moreno, G., Ramos-Román, M.J., García-Alix, A., Toney, J.L., Anderson, R.S., Jiménez-Espejo, F., Bright, J., Webster, C. & Yanes, Y. (2019) Vegetation and climate changes during the last two glacial-interglacial cycles in the western Mediterranean: a new long pollen record from Padul (southern Iberian Peninsula). *Quaternary Science Reviews*, 205, 86–105.

Camuera, J., Ramos-Román, M.J., Jiménez-Moreno, G., García-Alix, A., Ilvonen, L., Ruha, L., Gil-Romera, G., González-Sampériz, P. & Seppä, H. (2022) Past 200 kyr hydroclimate variability in the western Mediterranean and its connection to the African Humid Periods. *Scientific Reports*, 12(1), 9050.

Cohen, A.S. (2003) *Paleolimnology: the history and evolution of lake systems*. Oxford: Oxford University Press.

Combourieu Nebout, N., Peyron, O., Dormoy, I., Desprat, S., Beaudouin, C., Kotthoff, U. & Marret, F. (2009) Rapid climatic variability in the west Mediterranean during the last 25 000 years from high resolution pollen data. *Climate of the Past*, 5(3), 503–521.

Dansgaard, W., Johnsen, S., Clausen, H., Dahl-Jensen, D., Gundestrup, N., Hammer, C. & Oeschger, H. (1984) North Atlantic climatic oscillations revealed by deep Greenland ice cores. In: *Climate processes and climate sensitivity*, Vol. 29. Washington, DC: American Geophysical Union, pp. 288–298.

Davies, S.J., Lamb, H.F. & Roberts, S.J. (2015) Micro-XRF core scanning in palaeolimnology: recent developments. In: *Micro-XRF studies of sediment cores: Applications of a non-destructive tool for the environmental sciences*. Dordrecht: Springer, pp. 189–226.

De Deckker, P. & Last, W.M. (1989) Modern, non-marine dolomite in evaporitic playas of western Victoria, Australia. *Sedimentary Geology*, 64(4), 223–238.

De Deckker, P.D. & Last, W.M. (1988) Modern dolomite deposition in continental, saline lakes, western Victoria, Australia. *Geology*, 16(1), 29–32.

DiLoreto, Z.A., Bontognali, T.R., Al Disi, Z.A., Al-Kuwari, H.A.S., Williford, K.H., Strohmenger, C.J., Sadooni, F., Palermo, C., Rivers, J.M. & McKenzie, J.A. (2019) Microbial community composition and dolomite formation in the hypersaline microbial mats of the Khor Al-Adaid sabkhas, Qatar. *Extremophiles*, 23, 201–218.

Diloreto, Z.A., Garg, S., Bontognali, T.R. & Dittrich, M. (2021) Modern dolomite formation caused by seasonal cycling of oxygenic phototrophs and anoxygenic phototrophs in a hypersaline sabkha. *Scientific Reports*, 11(1), 4170.

Eugster, H. (1982) Climatic significance of lake and evaporite deposits. In: *Climate in Earth History: Studies in Geophysics*. Washington, DC: National Academy Press, pp. 105–111.

Faegri, K., Iversen, J., Kaland, P.E. & Krzywinski, K. (1989) *Textbook of pollen analysis*. Caldwell, NJ: Blackburn Press.

Fletcher, W., Sanchez Goñi, M., Peyron, O. & Dormoy, I. (2010) Abrupt climate changes of the last deglaciation detected in a Western Mediterranean forest record. *Climate of the Past*, 6, 245–264.

García-Alix, A., Jiménez-Moreno, G., Gázquez, F., Monedero-Contreras, R., López-Avilés, A., Jiménez-Espejo, F.J., Rodríguez-Rodríguez, M., Camuera, J., Ramos-Román, M.J. & Anderson, R.S. (2022) Climatic control on the Holocene hydrology of a playa-lake system in the western Mediterranean. *Catena*, 214, 106292.

Gierlowski-Kordesch, E.H. (2010) Lacustrine carbonates. *Developments in Sedimentology*, 61, 1–101.

Gil-Márquez, J.M., Andreo, B. & Mudarra, M. (2022) Studying hydrogeochemical processes to understand hydrodiversity and the related natural and cultural heritage. The case of Los Hoyos area (South Spain). *Catena*, 216, 106422.

Giralt, S., Burjachs, F., Roca, J. & Julià, R. (1999) Late Glacial to Early Holocene environmental adjustment in the Mediterranean semi-arid zone of the Salines playa-lake (Alacant, Spain). *Journal of Paleolimnology*, 21, 449–460.

Girela, L.L. & Martos, M.R. (1998) La laguna de Fuente de Piedra (Málaga), un área endorreica de interés ecológico ligada al karst yesífero-salino. In: *Karst en andalucía*. Madrid: Instituto Tecnologico Geiminero de Espana, pp. 165.

González-Sampériz, P., Valero-Garcés, B.L., Moreno, A., Jalut, G., García-Ruiz, J.M., Martí-Bono, C., Delgado-Huertas, A., Navas, A., Otto, T. & Dedoubat, J. (2006) Climate variability in the Spanish Pyrenees during the last 30,000 yr revealed by the El Portalet sequence. *Quaternary Research*, 66(1), 38–52.

Heinrich, H. (1988) Origin and consequences of cyclic ice rafting in the northeast Atlantic Ocean during the past 130,000 years. *Quaternary Research*, 29(2), 142–152.

Heredia, J., Araguás-Araguás, L. & Ruiz, J.M. (2004) Use of environmental tracers to characterize a complex hydrogeological system under variable density conditions: case of the subsurface brine of Fuente de Piedra (SW Spain). *Cartagena*, 18, 679–692.

Höbig, N., Mediavilla, R., Gibert, L., Santisteban, J.I., Cendón, D.I., Ibáñez, J. & Reicherter, K. (2016) Palaeohydrological evolution and implications for palaeoclimate since the Late Glacial at Laguna de Fuente de Piedra, southern Spain. *Quaternary International*, 407, 29–46.

Jiménez-Bonilla, A., Martegani, L., Rodríguez-Rodríguez, M., Gázquez, F., Díaz-Azpíroz, M., Martos, S., Reicherter, K. & Expósito, I. (2024) The role of neotectonics and climate variability in the Pleistocene-to-Holocene hydrological evolution of the Fuente de Piedra playa lake (southern Iberian Peninsula). *Hydrology and Earth System Sciences*, 28(23), 5311–5329.

Jiménez-Moreno, G., López-Avilés, A., García-Alix, A., Ramos-Román, M.J., Camuera, J., Mesa-Fernández, J.M., Jiménez-Espejo, F.J., López-Blanco, C., Carrión, J.S. & Anderson, R.S. (2023) Laguna Seca sediments reveal environmental and climate change during the latest Pleistocene and Holocene in Sierra Nevada, southern Iberian Peninsula. *Palaeogeography, Palaeoclimatology, Palaeoecology*, 631, 111834.

Joannin, S., Bassinot, F., Nebout, N.C., Peyron, O. & Beaudouin, C. (2011) Vegetation response to obliquity and precession forcing during the Mid-Pleistocene Transition in Western Mediterranean region (ODP site 976). *Quaternary Science Reviews*, 30(3–4), 280–297.

Kohfahl, C., Rodriguez, M., Fenk, C., Menz, C., Benavente, J., Hubberten, H., Meyer, H., Paul, L., Knappe, A. & López-Geta, J.A. (2008) Characterising flow regime and interrelation between surface-water and ground-water in the Fuente de Piedra salt lake basin by means of stable isotopes, hydrogeochemical and hydraulic data. *Journal of Hydrology*, 351(1–2), 170–187.

Land, L.S. (1998) Failure to Precipitate Dolomite at 25 C from Dilute Solution Despite 1000-Fold Oversaturation after 32 Years. *Aquatic Geochemistry*, 4(3), 361–368.

Last, W.M. (1990) Lacustrine dolomite—an overview of modern, Holocene, and Pleistocene occurrences. *Earth-Science Reviews*, 27(3), 221–263.

Lhénaff, R. (1981) *Recherches géomorphologiques sur les Cordillères Bétiques centro-occidentales (Espagne)*. Service de reproduction des theses. Université de Lille.

López-Avilés, A., Jiménez-Moreno, G., García-Alix, A., García-García, F., Camuera, J., Anderson, R.S., Sanjurjo-Sánchez, J., Chamorro, C.A. & Carrión, J.S. (2022) Post-glacial evolution of alpine environments in the western Mediterranean region: The Laguna Seca record. *Catena*, 211, 106033.

Mackenzie, F.T., Bischoff, W.D., Bishop, F.C., Loijens, M., Schoonmaker, J. & Wollast, R. (1983) Magnesian calcites; low-temperature occurrence, solubility and solid-solution behavior. *Reviews in Mineralogy and Geochemistry*, 11(1), 97–144.

Martín-Puertas, C., Valero-Garcés, B.L., Brauer, A., Mata, M.P., Delgado-Huertas, A. & Dulski, P. (2009) The Iberian–Roman humid period (2600–1600 cal yr BP) in the Zoñar Lake varve record (Andalucía, southern Spain). *Quaternary Research*, 71(2), 108–120.

Martín-Puertas, C., Valero-Garcés, B.L., Pilar Mata, M., González-Sampériz, P., Bao, R., Moreno, A. & Stefanova, V. (2008) Arid and humid phases in southern Spain during the last 4000 years: the Zoñar Lake record, Córdoba. *The Holocene*, 18(6), 907–921.

Martrat, B., Grimalt, J.O., Lopez-Martinez, C., Cacho, I., Sierro, F.J., Flores, J.A., Zahn, R., Canals, M., Curtis, J.H. & Hodell, D.A. (2004) Abrupt temperature changes in the Western Mediterranean over the past 250,000 years. *Science*, 306(5702), 1762–1765.

Meyers, P.A. (1997) Organic geochemical proxies of paleoceanographic, paleolimnologic, and paleoclimatic processes. *Organic Geochemistry*, 27(5–6), 213–250.

Meyers, P.A. & Lallier-Vergès, E. (1999) Lacustrine sedimentary organic matter records of Late Quaternary paleoclimates. *Journal of Paleolimnology*, 21, 345–372.

Montalván, F.J., Heredia, J., Ruíz, J.M., Pardo-Igúzquiza, E., de Domingo, A.G. & Elorza, F.J. (2017) Hydrochemical and isotopes studies in a hypersaline wetland to define the hydrogeological conceptual model: Fuente de Piedra Lake (Malaga, Spain). *Science of the Total Environment*, 576, 335–346.

Moreno, A., López-Merino, L., Leira, M., Marco-Barba, J., González-Sampériz, P., Valero-Garcés, B.L., López-Sáez, J.A., Santos, L., Mata, P. & Ito, E. (2011) Revealing the last 13,500 years of environmental history from the multiproxy record of a mountain lake (Lago Enol, northern Iberian Peninsula). *Journal of Paleolimnology*, 46, 327–349.

Ortiz, J.E., Torres, T., Delgado, A., Llamas, J., Soler, V., Valle, M., Julià, R., Moreno, L. & Díaz-Bautista, A. (2010) Palaeoenvironmental changes in the Padul Basin (Granada, Spain) over the last 1 Ma based on the biomarker content. *Palaeogeography, Palaeoclimatology, Palaeoecology*, 298(3–4), 286–299.

Pedrera, A., Martos-Rosillo, S., Galindo-Zaldívar, J., Rodríguez-Rodríguez, M., Benavente, J., Martín-Rodríguez, J. & Zúñiga-López, M. (2016) Unravelling aquifer-wetland interaction using CSAMT and gravity methods: the Mollina-Camorra aquifer and the Fuente de Piedra playa-lake, southern Spain. *Journal of Applied Geophysics*, 129, 17–27.

Pérez, A., Luzón, A., Roc, A., Soria, A., Mayayo, M. & Sánchez, J. (2002) Sedimentary facies distribution and genesis of a recent carbonate-rich saline lake: Gallocanta Lake, Iberian Chain, NE Spain. *Sedimentary Geology*, 148(1–2), 185–202.

Pourali, M., Sepehr, A., Hosseini, Z. & Hamzeh, M.A. (2023) Sedimentology, geochemistry, and geomorphology of a dry-lake playa, NE Iran: implications for paleoenvironment. *Carbonates and Evaporites*, 38(1), 9.

Queralt, I., Julia, R., Plana, F. & Bischoff, J.L. (1997) A hydrous Ca-bearing magnesium carbonate from playa lake sediments, Salines Lake, Spain. *American Mineralogist*, 82(7–8), 812–819.

Ramos-Román, M.J., Jiménez-Moreno, G., Camuera, J., García-Alix, A., Anderson, R.S., Jiménez-Espejo, F.J., Sachse, D., Toney, J.L., Carrión, J.S. & Webster, C. (2018) Millennial-scale cyclical environment and climate variability during the Holocene in the western Mediterranean region deduced from a new multiproxy analysis from the Padul record (Sierra Nevada, Spain). *Global and Planetary Change*, 168, 35–53.

Reading, H.G. (2009) *Sedimentary environments: processes, facies and stratigraphy*. Hoboken: John Wiley & Sons.

Reed, J.M., Stevenson, A.C. & Juggins, S. (2001) A multi-proxy record of Holocene climatic change in southwestern Spain: the Laguna de Medina, Cádiz. *The Holocene*, 11(6), 707–719.

Reimer, P.J., Austin, W.E., Bard, E., Bayliss, A., Blackwell, P.G., Ramsey, C.B., Butzin, M., Cheng, H., Edwards, R.L. & Friedrich, M. (2020) The IntCal20 Northern Hemisphere radiocarbon age calibration curve (0–55 cal kBP). *Radiocarbon*, 62(4), 725–757.

Rodrigo-Gámiz, M., Martínez-Ruiz, F., Jiménez-Espejo, F., Gallego-Torres, D., Nieto-Moreno, V., Romero, O. & Ariztegui, D. (2011) Impact of climate variability in the western Mediterranean during the last 20,000 years: oceanic and atmospheric responses. *Quaternary Science Reviews*, 30(15–16), 2018–2034.

Rodriguez-Rodriguez, M., Martos-Rosillo, S. & Pedrera, A. (2016) Hydrogeological behaviour of the Fuente-de-Piedra playa lake and tectonic origin of its basin (Malaga, southern Spain). *Journal of Hydrology*, 543, 462–476.

Rodríguez-Rodríguez, M., Benavente, J., Cruz-San Julián, J. & Martos, F.M. (2006) Estimation of ground-water exchange with semi-arid playa lakes (Antequera region, southern Spain). *Journal of Arid Environments*, 66(2), 272–289.

Rodríguez-Rodríguez, M., Benavente, J. & Moral, F. (2005) High density ground-water flow, major-ion chemistry and field experiments in a closed basin: Fuente de Piedra Playa Lake (Spain). *American Journal of Environmental Sciences*, 1(2), 164–171.

Rodríguez-Rodríguez, M., Pedrera, A., Cruz, M. & Martos, S. (2016b) Applying piezometric evolution indicators to facilitate stakeholderâ s participation in the management of groundwater-dependent ecosystems. Case study: Fuente de Piedra playa lake (southern Spain). *Hydrobiologia*, 782, 145–154.

Rosen, M.R., Miser, D.E., Starcher, M.A. & Warren, J.K. (1989) Formation of dolomite in the Coorong region, South Australia. *Geochimica et Cosmochimica Acta*, 53(3), 661–669.

Sadooni, F., Howari, F. & El-Saiy, A. (2010) Microbial dolomites from carbonate-evaporite sediments of the coastal sabkha of Abu Dhabi and their exploration implications. *Journal of Petroleum Geology*, 33(4), 289–298.

Sánchez-Román, M., Chandra, V., Mulder, S., Areias, C., Reijmer, J. & Vahrenkamp, V. (2025) The hidden role of heterotrophic bacteria in early carbonate diagenesis. *Scientific Reports*, 15(1), 561.

Sánchez-Román, M., Gibert, L., Martín-Martín, J.D., van Zuilen, K., Pineda-González, V., Vroon, P. & Bruggmann, S. (2023) Sabkha and salina dolomite preserves the biogeochemical conditions of its depositional paleoenvironment. *Geochimica et Cosmochimica Acta*, 356, 66–82.

Sánchez-Román, M., McKenzie, J.A., Wagener, A.d.L.R., Rivadeneyra, M.A. & Vasconcelos, C. (2009b) Presence of sulfate does not inhibit low-temperature dolomite precipitation. *Earth and Planetary Science Letters*, 285(1–2), 131–139.

Sánchez-Román, M., McKenzie, J.A., Wagener, A.d.L.R., Romanek, C.S., Sánchez-Navas, A. & Vasconcelos, C. (2011a) Experimentally determined biomediated Sr partition coefficient for dolomite: significance and implication for natural dolomite. *Geochimica et Cosmochimica Acta*, 75(3), 887–904.

Sánchez-Román, M., Romanek, C.S., Fernández-Remolar, D.C., Sánchez-Navas, A., McKenzie, J.A., Pibernat, R.A. & Vasconcelos, C. (2011b) Aerobic biomineralization of Mg-rich carbonates: implications for natural environments. *Chemical Geology*, 281(3–4), 143–150.

Sánchez-Román, M., Vasconcelos, C., Schmid, T., Dittrich, M., McKenzie, J.A., Zenobi, R. & Rivadeneyra, M.A. (2008) Aerobic microbial dolomite at the nanometer scale: implications for the geologic record. *Geology*, 36(11), 879–882.

Sánchez-Román, M., Vasconcelos, C., Warthmann, R., Rivadeneyra, M. & McKenzie, J.A. (2009a) Microbial dolomite precipitation

under aerobic conditions: results from Brejo do Espinho Lagoon (Brazil) and culture experiments. In: *Perspectives in carbonate geology: a tribute to the career of Robert Nathan Ginsburg*. Oxford: Wiley, pp. 167–178.

Sanz de Galdeano, C., Lozano, J. & Puga, E. (2008) Structure and organization of Trias from Antequera. *Revista de la Sociedad Geológica de España*, 21(3–4), 111–124.

Schröder, T., Van't Hoff, J., Ortiz, J.E., de Torres Pèrez-Hidalgo, T.J., López-Sáez, J.A., Melles, M., Holzhausen, A., Wennrich, V., Viehberg, F. & Reicherter, K. (2018a) Shallow hypersaline lakes as paleoclimate archives: a case study from the Laguna Salada, Málaga province, southern Spain. *Quaternary International*, 485, 76–88.

Schroeder, T., van't Hoff, J., López-Sáez, J.A., Viehberg, F., Melles, M. & Reicherter, K. (2018b) Holocene climatic and environmental evolution on the southwestern Iberian Peninsula: a high-resolution multi-proxy study from Lake Medina (Cádiz, SW Spain). *Quaternary Science Reviews*, 198, 208–225.

Stuiver, M. & Reimer, P.J. (1993) Extended 14C data base and revised CALIB 3.0 14C age calibration program. *Radiocarbon*, 35(1), 215–230.

Valero-Garcés, B., Navas, A., Mata, P., Delgado-Huertas, A., Machín, J., González-Sampériz, P., Moreno Caballud, A., Schwalb, A., Ariztegui, D. & Schnellmann, M. (2003) Sedimentary facies analyses in lacustrine cores: from initial core descriptions to detailed paleoenvironmental reconstructions. A case study from Zoñar Lake (Cordoba province, Spain). In: *Limnogeology in Spain: a tribute to Kerry Kelts*. Madrid: Consejo Superior de Investigaciones Cientificas, pp. 385–414.

Valero-Garcés, B.L., Delgado-Huertas, A., Navas, A., MachÍn, J., González-Sampériz, P. & Kelts, K. (2000) Quaternary palaeohydrological evolution of a playa lake: Salada Mediana, central Ebro Basin, Spain. *Sedimentology*, 47(6), 1135–1156.

Valero-Garcés, B.L., González-Sampériz, P., Navas, A., Machín, J., Mata, P., Delgado-Huertas, A., Bao, R., Moreno, A., Carrión, J.S. & Schwalb, A. (2006) Human impact since medieval times and recent ecological restorationin a Mediterranean lake: the laguna Zoñar, southern Spain. *Journal of Paleolimnology*, 35, 441–465.

Vasconcelos, C. & McKenzie, J.A. (1997) Microbial mediation of modern dolomite precipitation and diagenesis under anoxic conditions (Lagoa Vermelha, Rio de Janeiro, Brazil). *Journal of Sedimentary Research*, 67(3), 378–390.

Vegas, J., Ruiz-Zapata, B., Ortiz, J.E., Galán, L., Torres, T., García-Cortés, Á., Gil-García, M.J., Pérez-González, A. & Gallardo-Millán, J.L. (2010) Identification of arid phases during the last 50 cal. ka BP from the Fuentillejo maar-lacustrine record (Campo de Calatrava Volcanic Field, Spain). *Journal of Quaternary Science*, 25(7), 1051–1062.

Warren, J. (2000) Dolomite: occurrence, evolution and economically important associations. *Earth-Science Reviews*, 52(1–3), 1–81.

Warren, J.K. (2016) Sabkhas, saline mudflats and pans. In: *Evaporites: A Geological Compendium*. Cham: Springer, pp. 207–301.

Wright, D.T. (1999) The role of sulphate-reducing bacteria and cyanobacteria in dolomite formation in distal ephemeral lakes of the Coorong region, South Australia. *Sedimentary Geology*, 126(1–4), 147–157.

SUPPORTING INFORMATION

Additional supporting information can be found online in the Supporting Information section at the end of this article.

How to cite this article: Naim, Z., Li, G., Gibert, L., Stuut, J.-B., Jiménez-Moreno, G. & Sánchez-Román, M. (2025) Laguna Fuente de Piedra: An example of a dolomite factory recording ~50,000 years of depositional and paleoclimatic evolution. *The Depositional Record*, 00, 1–20. Available from: https://doi.org/10.1002/dep2.70052